Journal for Geometry and Graphics
Volume 16 (2012), No. 2, 223–234.

Design of Infinitesimally and Finitely Flexible Origami Based on Reciprocal Figures

Tomohiro Tachi

Graduate School of Arts and Sciences, The University of Tokyo
3-8-1 Komaba, Meguro-Ku, Tokyo 153-8902, Japan
email: tachi@idea.c.u-tokyo.ac.jp

Abstract. This paper investigates novel computational design method for infinitesimally and finitely foldable rigid origami based on solving a first-order folding mode, which can be represented by a reciprocal figure. We derive these graphical conditions from a matrix representation of rigid origami, and extend the conditions to cases when the surface includes holes. We propose an algorithm to obtain forms that satisfy the conditions and an interactive system to freely design infinitesimally foldable forms. We show design examples of shaky polyhedron and origami, and finitely foldable quadrivalent mesh origami.

Key Words: Origami, rigid origami, infinitesimal flexibility, shaky polyhedron, reciprocal figure

MSC 2010: 52C25, 52B10, 52B70, 53A17

1. Introduction

Rigid origami is a polyhedral origami modeled using rigid panels and rotational hinges. The designs of mechanisms and the structures based on the kinematic property of rigid origami are interesting topics in the field of origami engineering, since they can facilitate applications of deployable structures and flexible meta-material at different scales, e.g., from medical devices inside the human body to architectural and space structures. From a theoretical viewpoint, rigid origami structures are especially interesting when they acquire flexibility from redundant mechanical constraints based on their non-trivial singular geometric configuration, such as flexible closed polyhedra and rigid-foldable quadrivalent mesh origami structures. In designs using rigid origami mechanisms, such redundancies can be used for removing a part of the structure without disturbing the mechanism or combining multiple compatible parts to form more complex and robust structures.

Infinitesimal and finite kinematic properties of polyhedral surfaces have been studied theoretically and have also been associated with reciprocal figures in 3D, specifically reciprocal-parallel, by Sauer [6] for quadrangle meshes. Schief et al. [7] studied reciprocal figures that

ISSN 1433-8157/$ 2.50

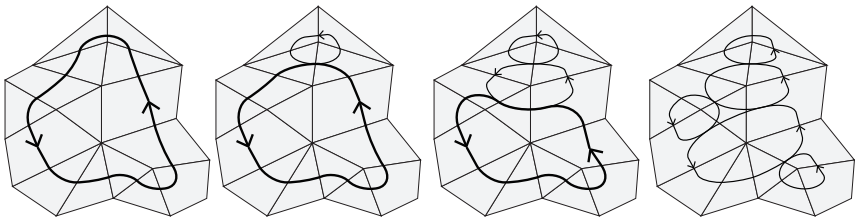

Figure 1: Contraction of a closed loop. This also implies that a non-simply connected surface requires additional treatment.

also have second-order flexibility. Redundant finite mechanisms have been studied as well, e.g., flexibility of closed polyhedra [3] and flexibility of quad panel meshes [7, 9, 8]. Despite these theoretical studies, design methods of such structures are limited. A computational system for bi-directionally flat-foldable quad mesh origami [9] facilitates interactive formfinding of finitely foldable rigid origami structures with redundant constraints. The drawback of this method is that the system relies on the existence of a valid state in a half-folded form.

In this paper, we propose a novel design method for obtaining infinitesimally and finitely transformable origami and polyhedral surfaces by developing an interactive design system that solves the condition of the existence of an infinitesimal folding mode, which can be graphically represented by a reciprocal figure.

In Section 2, we derive the infinitesimal flexibility conditions for disk meshes equivalent to existing results [6, 7], using a matrix representation of transformation. Next we naturally extend the conditions to the case of a disk with holes by distinguishing conditions around each hole. In Section 3, we propose a computational method for obtaining a valid configuration and a reciprocal figure. We first obtain an initial configuration based on optimization and use the same system to explore possible solutions by projecting perturbation in the solution space. Using the system, we can obtain design variations of infinitesimally foldable closed polyhedron, as shown in Section 4. In Section 5, we apply a second-order flexibility condition represented by reciprocal figure to a bi-directionally flat-foldable quadrivalent 2D crease pattern. Despite the lack of a proof, we observed that this condition yields finitely rigid-foldable origami patterns. One of the results is "curved rigid origami", which is a discretization of the curved folding that acts as a one-degree-of-freedom (1-DOF) mechanism.

2. Infinitesimal folding mode and reciprocal figure

A rigid origami structure comprises rigid panels and hinge joints at the foldlines, and can be modeled like a robot arm; however it has many closed loops. The constraints of its overall mechanism can be described using matrix equations as in [4, 2], which are redundantly given for any possible sequence of foldlines forming a closed-loop strip. Here, we will focus only on the kinematics and ignore self-collision.

In the case of a rigid origami model that is homeomorphic to a disk, it is sufficient to consider only the constraints resulting from the closed faceted fan around each interior vertex. This is because any loop condition decompose into a contracted loop condition and an interior vertex condition, which further decomposes into multiple interior vertex conditions after several iterations (Fig. 1). This implies that this condition is sufficiently applicable to a simply connected 2-manifold.

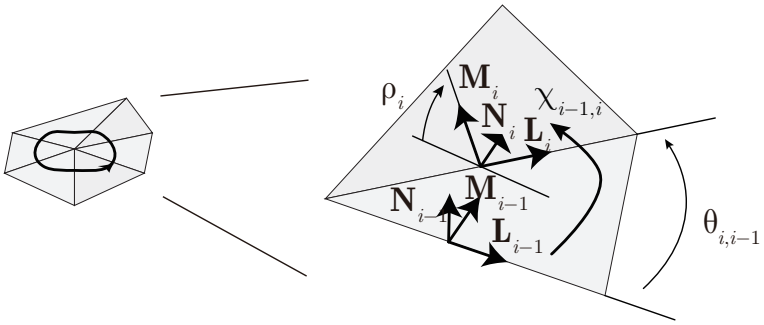

Figure 2: Rotation around a fan.

Single-vertex constraint The constraint along the fan around an interior vertex is described as follows. Let the fold angle of the vertex's incident foldline i be denoted by ρ_i and the angle between adjacent foldlines i and $i+1$ be denoted by $\theta_{i,i+1}$. Here, note that there are n incident foldlines incrementally numbered counterclockwise, and their index is numbered in modulo n. Then, the rotation by foldline i is described by a 3×3 matrix $\chi_{i-1,i}$, which transforms the local coordinate of a facet $i-1, i$ to that of facet $i, i+1$. Let the local coordinate of facet $i-1, i$ have its x and z axes along the foldline and the facet's normal, respectively. $\chi_{i-1,i}$ is represented as the sequence of a pitch and then yaw (Fig. 2).

$$\chi_{i-1,i} = \mathbf{Y}_{i-1,i}\mathbf{P}_i = \begin{bmatrix} \cos\theta_{i-1,i} & -\sin\theta_{i-1,i} & 0 \\ \sin\theta_{i-1,i} & \cos\theta_{i-1,i} & 0 \\ 0 & 0 & 1 \end{bmatrix} \begin{bmatrix} 1 & 0 & 0 \\ 0 & \cos\rho_i & -\sin\rho_i \\ 0 & \sin\rho_i & \cos\rho_i \end{bmatrix}. \tag{1}$$

In order to maintain consistency as a closed fan, sequentially applying the rotations around the closed loop must transform the orientation of the first facet, i.e., $0, 1$ to be identical to its original orientation.

$$\mathbf{R}\left(\rho_0, \cdots, \rho_{n-1}\right) = \chi_{0,1}\chi_{1,2}\cdots\chi_{n-1,0} = \mathbf{I}. \tag{2}$$

Infinitesimal motion The derivative of the constraint with respect to ρ_i is calculated as follows. Define an orthogonal matrix $\mathbf{T}_i$ representing the orientation of the facet $i, i+1$ with respect to the facet $0, 1$ as

$$\mathbf{T}_i = \chi_{0,1}\cdots\chi_{i-1,i} = \begin{bmatrix} \mathbf{L}_i & \mathbf{M}_i & \mathbf{N}_i \end{bmatrix} = \begin{bmatrix} L_i^x & M_i^x & N_i^x \\ L_i^y & M_i^y & N_i^y \\ L_i^z & M_i^z & N_i^z \end{bmatrix},$$

where $\mathbf{L}_i$ is the direction vector of edge i and $\mathbf{N}_i$ is the normal of facet $i, i+1$ with respect to the local coordinate system whose x and z axes orient the direction of foldline 0 and the normal of facet $0, 1$. Then, Eq. (2) is written as $\mathbf{R} = \begin{bmatrix}\mathbf{T}_i\end{bmatrix}\begin{bmatrix}\mathbf{T}_i\end{bmatrix}^{\mathsf{T}} = \mathbf{I}$. By using

$$\frac{\partial\chi_{i-1,i}}{\partial\rho_i} = \left(\mathbf{Y}_{i-1,i}\mathbf{P}_i\right)\mathbf{P}_i^{-1}\frac{\partial\mathbf{P}_i}{\partial\rho_i} = \chi_{i-1,i}\begin{bmatrix} 0 & 0 & 0 \\ 0 & 0 & -1 \\ 0 & 1 & 0 \end{bmatrix},$$

we obtain the derivative of Eq. (2) as

$$\frac{\partial\mathbf{R}}{\partial\rho_i} = \begin{bmatrix}\mathbf{T}_i\end{bmatrix}\begin{bmatrix} 0 & 0 & 0 \\ 0 & 0 & -1 \\ 0 & 1 & 0 \end{bmatrix}\begin{bmatrix}\mathbf{T}_i\end{bmatrix}^{\mathsf{T}} = \begin{bmatrix} 0 & -L_i^z & L_i^y \\ L_i^z & 0 & -L_i^x \\ -L_i^y & L_i^x & 0 \end{bmatrix}. \tag{3}$$

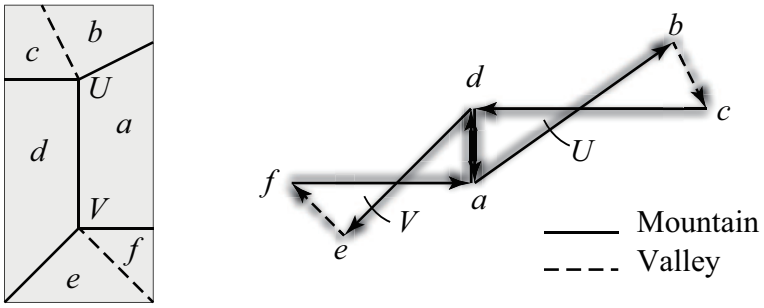

Figure 3: Left: A foldline network. Right: A reciprocal figure of the foldline network. The illustration shows the planar case with zero signed area (Section 2.2).

The constraints can be written using three independent equations:

$$\mathbf{f} = \begin{bmatrix} \mathbf{R}(2,3) \\ \mathbf{R}(3,1) \\ \mathbf{R}(1,2) \end{bmatrix} = \mathbf{0}. \tag{4}$$

The infinitesimal folding motion $(\Delta\rho_1, \cdots, \Delta\rho_n)$ satisfies

$$\sum_{i=0}^{n-1} \frac{\partial \mathbf{f}}{\partial \rho_i} \Delta\rho_i = \sum_{i=0}^{n-1} \mathbf{L}_i \Delta\rho_i = \mathbf{0}. \tag{5}$$

Here, $\mathbf{L}_i$ is the normalized direction vector of edge i from a vertex to the adjacent vertex in the local coordinate system of facet $0, 1$.

Now, we consider the global system given by the intersection of the constraints from each interior vertex. We denote the position of vertex v $(v = 1, \cdots, V)$ by $\mathbf{x}_v$, and the rotation along the foldline incident to vertex u and v by $\rho_{u,v} = \rho_{v,u}$ or ρ_e $(e = 1, \cdots, E_{\text{in}})$, where V and E_{in} are the numbers of total vertices and fold lines respectively. For later convenience, we let $1, \cdots, V_{\text{in}}$ be the interior vertices and $V_{\text{in}} + 1, \cdots, V$ be the exterior vertices, where V_{in} is the number of interior vertices.

We apply a rotation $\mathbf{T}_u$ to Eq. (5) so that for any edge u, v, $\mathbf{L}'_{u,v} = \mathbf{T}_u \mathbf{L}^{u,v}$ is the direction vector of the edge in the global coordinate system, i.e., $\dfrac{\partial \mathbf{f}'_u}{\partial \rho_{u,v}} = \mathbf{L}'_{u,v} = (\mathbf{x}_u - \mathbf{x}_v) \,/\, \|\mathbf{x}_u - \mathbf{x}_v\|$. The infinitesimal folding motion satisfies, for each interior vertex $v = 1, \ldots, V_{\text{in}}$,

$$\sum_{u \text{ adjacent to } v} \frac{(\mathbf{x}_u - \mathbf{x}_v)}{\|\mathbf{x}_u - \mathbf{x}_v\|} \Delta\rho_{u,v} = \mathbf{0}. \tag{6}$$

Reciprocal figure This equation is equivalent to an equilibrium condition when $\Delta\rho_{u,v}$ is replaced by the axial force applied to the lines. As in the field of graphical statics where reciprocal figures have been used to solve an equilibrium of a 2D frameworks [5, 1], we consider a 3D reciprocal figure of origami foldlines.

Because we are interested in a 3D reciprocal figure, we consider reciprocal figures to be the dual graph of a foldline network in 3D space whose corresponding edges are parallel (instead of perpendicular), i.e., "reciprocal-parallel" as defined by Sauer [6]. The dual graph is constructible because the origami surface is a manifold; and the interior vertex, foldlines, and facets of the polyhedral surface correspond to polygons, segments, and nodes, respectively. Here, note that we use only foldlines (edges between facets) but not boundary edges (Fig. 3).

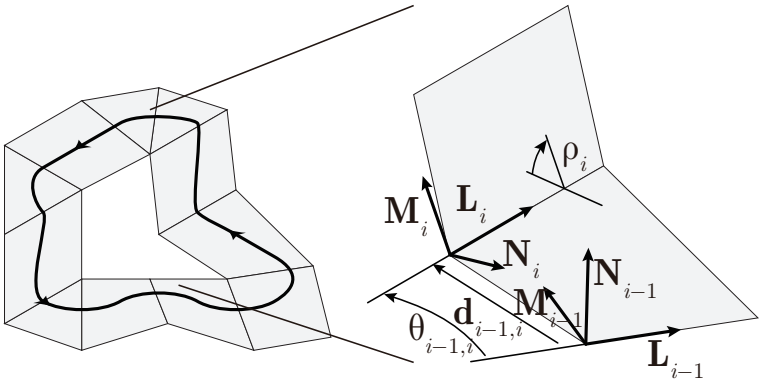

Figure 4: Rotation around a hole.

Theorem 1 (Schief et al. [7]). *The existence of a (non-degenerate) reciprocal figure of the foldline network of a rigid origami structure homeomorphic to a disk is equivalent to the existence of a first-order folding mode of the rigid origami structure.*

Proof: Assume that a valid first order folding motion exists. Then, we construct a dual graph of the foldline network such that the node coordinate $\mathbf{x}'_f$ is the angular velocity of the corresponding facet f. For each adjacent pair of facets f and g and the foldline u, v between them, $\mathbf{x}'_f - \mathbf{x}'_g = \dfrac{(\mathbf{x}_u - \mathbf{x}_v)}{\|\mathbf{x}_u - \mathbf{x}_v\|}\Delta\rho_{u,v}$; thus, the graph is a reciprocal figure of the foldline network.

Similarly, assume that a reciprocal figure of the foldline network exists, in which the coordinate of the node corresponding to facet f is denoted by $\mathbf{x}'_f$. Then, we let the angular speed of each foldline u, v between facets f and g be $\|\mathbf{x}'_f - \mathbf{x}'_g\|$. This set of angular speeds of follines satisfies Eq. (6), thereby representing a valid infinitesimal folding motion. □

2.1. Surface with holes

Non-disk origami, or specifically non-simply connected origami, e.g., cylindrical origami or origami with holes, is often applied to obtain collapsible structures. The infinitesimal folding mode of an origami structure with holes can be represented by the intersection of constraints around each interior vertex and additional constraints for the loop around each hole. Unlike the constraint around a vertex, there are six constraints around a loop, which correspond to rotation and translation.

Similar to a single vertex, we represent transformation by matrices, but in this case, we use a 4×4 homogeneous matrix so that we can take both translation and rotation into account.

$$\chi_{i-1,i} = \mathbf{Y}_{i-1,i}\mathbf{P}_i = \begin{bmatrix} \cos\theta_{i-1,i} & -\sin\theta_{i-1,i} & 0 & d^x_{i-1,i} \\ \sin\theta_{i-1,i} & \cos\theta_{i-1,i} & 0 & d^y_{i-1,i} \\ 0 & 0 & 1 & 0 \\ 0 & 0 & 0 & 1 \end{bmatrix} \begin{bmatrix} 1 & 0 & 0 & 0 \\ 0 & \cos\rho_i & -\sin\rho_i & 0 \\ 0 & \sin\rho_i & \cos\rho_i & 0 \\ 0 & 0 & 0 & 1 \end{bmatrix}, \tag{7}$$

where $\mathbf{d}_{i-1,i} = \left(d^x_{i-1,i}, d^y_{i-1,i}, 0\right)^\mathsf{T}$ represents the origin point of facet $i, i+1$ observed from the local coordinate of $i-1, i$ (Fig. 4). Then, the orientation and position of facet $i, i+1$ with respect to facet $0, 1$ is

$$\mathbf{T}_i = \begin{bmatrix} \mathbf{L}_i & \mathbf{M}_i & \mathbf{N}_i & \mathbf{O}_i \\ 0 & 0 & 0 & 1 \end{bmatrix},$$

where $\mathbf{O}_i$ represents the position of the origin observed from facet $0, 1$. The derivative of Eq. (2) is calculated as

$$\frac{\partial \mathbf{R}}{\partial \rho_i} = \left[\begin{array}{ccc|c} 0 & -L_i^z & L_i^y & \\ L_i^z & 0 & L_i^x & \mathbf{L}_i \times \mathbf{O}_i \\ -L_i^y & L_i^x & 0 & \\ \hline \multicolumn{3}{c|}{\mathbf{0}} & 0 \end{array}\right]$$

We obtain six independent equations:

$$\mathbf{f} = \begin{bmatrix} \mathbf{R}(2,3) \\ \mathbf{R}(3,1) \\ \mathbf{R}(1,2) \end{bmatrix} = \mathbf{0} \quad \text{and} \quad \mathbf{g} = \begin{bmatrix} \mathbf{R}(1,4) \\ \mathbf{R}(2,4) \\ \mathbf{R}(3,4) \end{bmatrix} = \mathbf{0}.$$

Here, $\mathbf{f} = \mathbf{0}$ and $\mathbf{g} = \mathbf{0}$ represent the closure conditions of rotation and translation, respectively. We can similarly use a global coordinate system to replace $\mathbf{L}_i$ by $\mathbf{L}'_{u,v} = (\mathbf{x}_u - \mathbf{x}_v) \,/\, \|\mathbf{x}_u - \mathbf{x}_v\|$ and $\mathbf{O}_i$ by $\mathbf{O}'_u = \mathbf{x}_u$.

Since $\mathbf{f} = \mathbf{0}$ reduces to Eq. (6), the overall constraints for the infinitesimal folding motion are as follows.

1. For each interior vertex v and for each hole with incident foldlines u, v (v is on the boundary), Eq. (6) is satisfied and,
2. For each hole,

$$\sum_{\text{incident foldline } u,v} \left(\frac{(\mathbf{x}_u - \mathbf{x}_v)}{\|\mathbf{x}_u - \mathbf{x}_v\|} \Delta\rho_{u,v} \right) \times \mathbf{x}_v = \mathbf{0}. \tag{8}$$

Similarly to the case of disk origami, these equations are equivalent to an equilibrium condition when the hole is replaced by a rigid body. Here, Eqs. (6) and (8) represent the equilibrium of forces and moments, respectively.

A valid reciprocal figure of the foldline network can be constructed similarly to the case of a disk. However, the reciprocal figure is only a necessary condition for infinitesimal foldability, and is not a sufficient condition.

2.2. Conditions in degenerate planar surfaces

In the previous sections, we considered a polyhedral surface in general, which is not necessarily a developable surface, although the term "origami" typically implies developability. Developable origami surfaces can be manufactured just by folding a sheet of paper; in this process of manufacturing, the existence of folding motion matters. We have observed from examples that when we apply developability and flexibility conditions at the same time, the surface often converges to a completely flat state. When every vertex lies in a plane, the constraints given by a reciprocal figure degenerate, and one of the three constraints for each vertex is lost. In this case, the additional flexibility is not desirable since it represents no valid folding motion, but rather lends a trivial shakiness in the planar state.

In order to find a valid folding motion in the flat state, we apply the condition that the signed area of the cell in the reciprocal figure is zero as is introduced by Watanabe and Kawaguchi [11], as the second-order folding mode of origami in the flat state. This zero-area condition is represented as

$$\sum_{i=0}^{n-1} \sum_{j=0}^{i-1} \mathbf{L}_j \Delta\rho_j \times \mathbf{L}_i \Delta\rho_i = \mathbf{0}. \tag{9}$$

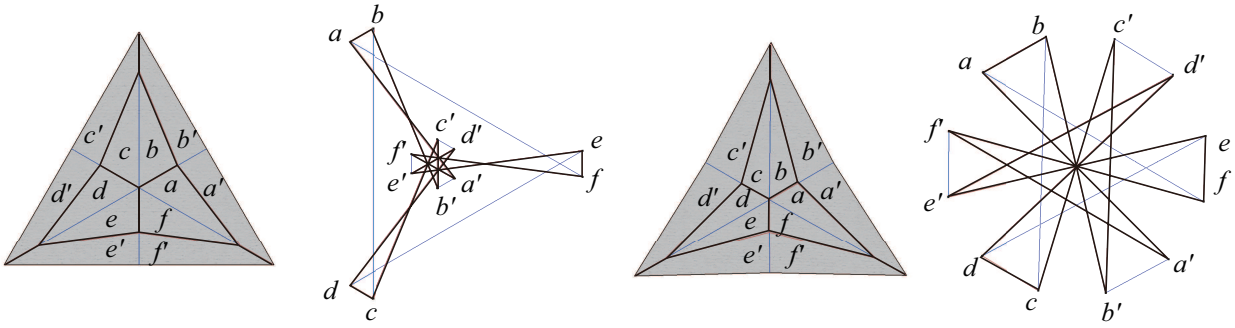

Figure 5: Left: A pattern without the zero-area condition. Note the asymmetric quadrangles and hexagons with positive- and negative- signed area. This pattern is a bistable structure when the panel is not triangulated. Right: Modified pattern with the zero-area condition. This pattern has second-order flexibility in a planar state.

Since $\mathbf{L}_i$ lies in a plane, the orientation of this vector is always kept perpendicular to the plane. Therefore, only one out of three equations is independent, and the vector orientation is always perpendicular to the constraints of Eq. (5). Therefore, the intersection of Eqs. (5) and (9) can be represented by their linear combination as

$$\sum_{i=0}^{n-1}\Big(\mathbf{L}_i\Delta\rho_i + \sum_{j=0}^{i-1}\mathbf{L}_j\Delta\rho_j \times \mathbf{L}_i\Delta\rho_i\Big) = \mathbf{0}. \tag{10}$$

Figure 5 shows example patterns with and without the zero-area conditions.

3. Computational method

We propose a novel interactive method for designing variations of infinitesimally foldable origami structures. The method is especially useful when achieving a flexible state of an origami structure in which the number of constraints exceeds the number of variables; this type of origami generically becomes a static structure. The configuration of an origami structure with an infinitesimal folding mode is represented by its vertex coordinates and reciprocal figure. We parameterize the configuration by the vertex coordinates $\mathbf{X} = \left(\mathbf{x}_1^\mathsf{T}, \cdots, \mathbf{x}_V^\mathsf{T}\right)^\mathsf{T}$ and the ratios $\mathbf{W} = (w_1, \cdots, w_{E_\mathrm{in}})^\mathsf{T}$ of the edges. Each element of $\mathbf{W}$ corresponding to edge e connecting vertices u, v is represented $w_e = \Delta\rho_e/\ell_e$. The constraints in Eq. (6) are re-written as

$$\Delta\mathbf{f}_v = \sum_{u \text{ incident to } v} w_{u,v}\left(\mathbf{x}_u - \mathbf{x}_v\right) = \mathbf{0} \tag{11}$$

Here, the sign of w_e indicates wheter the fold angle increases or decreases by the folding. In order to avoid the trivial solution that the angular velocity of every foldline equals 0, we set the following conditions:

$$\begin{cases} w_e < -\alpha & \text{folding mountain or unfolding valley,} \\ w_e > \alpha & \text{folding valley or unfolding mountain,} \end{cases} \tag{12}$$

where α can be set to an arbitrary positive value proportional to some scale factor.

Initial solution We solve Eqs. (11) and (12) by solving

$$U = \sum_{v=1}^{V_{\text{in}}} \|\Delta \mathbf{f}_v\|^2 + \sum_{e=1}^{E_{\text{in}}} \max\left(0, \alpha - |w_e|\right)^2 = 0$$

with respect to $\mathbf{X}$ and $\mathbf{W}$. The solution is not unique, and we find a solution close to the original configuration by the following two steps.

1. Minimize U with respect to $\mathbf{W}$ while $\mathbf{X}$ is fixed.
2. Minimize U with respect to $\mathbf{X}$ and $\mathbf{W}$ using the previous result as the initial configuration.

If $3V < E$ as in a triangular disk mesh, step 1 alone yields $U = 0$. An interesting case occurs when $3V \geq E$, e.g., quadrangle based origami pattern or a cylindrical or closed polyhedron, which suggests that the structure is generically static. The minimization problem in step 1 converges to the least square solution of an over-constrained system, and then the pattern is modified to a flexible configuration with singularity in step 2. For solving the above optimization problems, the conjugate gradient method is used.

Exploring solution space Once we obtain a solution, we can get variations of the patterns using a perturbation-based method that uses $\mathbf{F}(\mathbf{X}, \mathbf{W}) = \left\{\Delta \mathbf{f}_1^{\mathsf{T}}, \ldots, \Delta \mathbf{f}_{V_{\text{in}}}^{\mathsf{T}}\right\}^{\mathsf{T}} = \mathbf{0}$ as a geometric constraint that forms a multi-dimensional continuous solution space. A plausible deformation represented by $3V + E$-vector $[\Delta \mathbf{X} \quad \Delta \mathbf{W}]^{\mathsf{T}}$ must satisfy

$$[\mathbf{C}] \begin{bmatrix} \Delta \mathbf{X} \\ \Delta \mathbf{W} \end{bmatrix} = \begin{bmatrix} \dfrac{\partial \mathbf{F}}{\partial \mathbf{X}} & \dfrac{\partial \mathbf{F}}{\partial \mathbf{W}} \\ \dfrac{\partial \mathbf{G}}{\partial \mathbf{X}} & \dfrac{\partial \mathbf{G}}{\partial \mathbf{W}} \end{bmatrix} \begin{bmatrix} \Delta \mathbf{X} \\ \Delta \mathbf{W} \end{bmatrix} = \mathbf{0}, \tag{13}$$

where $\mathbf{G}$ represents other optional constraints such as the penalty constraints derived from Eq. (12), developability, and flat-foldability, i.e., the constraints combined with the constraints described in [10]. The elements are calculated as follows.

$$\frac{\partial \Delta \mathbf{f}_v}{\partial \mathbf{x}_u} = \begin{cases} -\sum_{k \text{ incident to } v} w_{v,k} & \text{if } u = v \\ w_{v,u} & \text{if } u \text{ is incident to } v \\ 0 & \text{else} \end{cases} \tag{14}$$

$$\frac{\partial \Delta \mathbf{f}_v}{\partial \mathbf{w}_{u,k}} = \begin{cases} \mathbf{x}_k - \mathbf{x}_v & \text{if } u = v \text{ (or } \mathbf{x}_u - \mathbf{x}_v \text{ if } v = k) \\ 0 & \text{else} \end{cases} \tag{15}$$

Equations (8) and (10) are polynomial functions of $w_{u,v}$ and $\mathbf{x}_u$; the derivative functions in these cases can be similarly calculated.

We apply the perturbation based method similar to [10] using the Moore-Penrose generalized inverse $\mathbf{C}^+$ of the constraint matrix $\mathbf{C}$ as follows:

$$\begin{bmatrix} \Delta \mathbf{X} \\ \Delta \mathbf{W} \end{bmatrix} = \left(\mathbf{I} - \mathbf{C}^+ \mathbf{C}\right) \begin{bmatrix} \Delta \mathbf{X}_0 \\ \Delta \mathbf{W}_0 \end{bmatrix}, \tag{16}$$

where $\begin{bmatrix} \Delta \mathbf{X}_0 \\ \Delta \mathbf{W}_0 \end{bmatrix}$ is an arbitrarily assigned initial deformation, which is projected orthogonally to the constrained subspace by multiplying with $(\mathbf{I} - \mathbf{C}^+ \mathbf{C})$; this results in a valid deformation that is as close as possible to the given initial deformation.

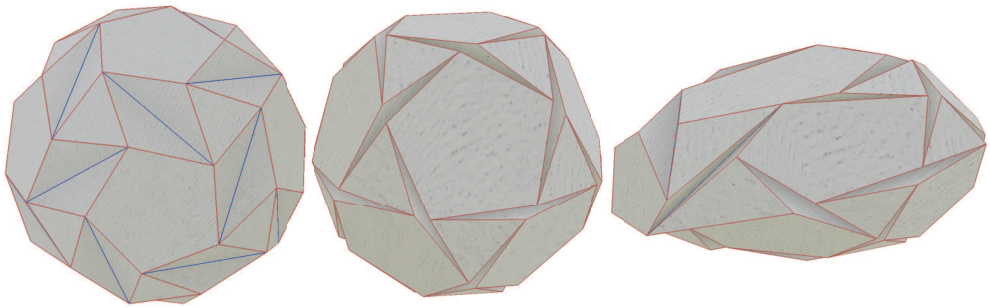

Figure 6: Left: A snub dodecahedron with flipped edges. Middle: A shaky polyhedron obtained by two-step optimization to satisfy the infinitesimal foldability condition. Right: The freeform variation wherein shakiness and planarity of the pentagonal facet are preserved.

We implemented the constraints and variables by improving freeform origami [10]. In this system, the user can freely select and drag points on the rendered origami structure through a 2D input device to apply a deformation, e.g., translation of a point or a weighed point-set translation or rotation. Before actually applying the deformation to the current state, the deformation vector $\begin{bmatrix}\Delta\mathbf{X}_0\\ \mathbf{0}\end{bmatrix}$ is substituted by $\begin{bmatrix}\Delta\mathbf{X}\\ \Delta\mathbf{W}\end{bmatrix}$ to obtain a constrained valid next state. Since the above-mentioned Euler's integration accumulates the error, the residual is eliminated based on Newton-Raphson's method for each step. The generalized inverse solution for each step is calculated using the conjugate gradient method. In this way, we immediately achieve a valid variation of forms in an interactive manner.

4. Shaky closed polyhedron

By using the system, we can design a variation of a shaky, i.e., infinitesimally transformable, closed polyhedron. Since the number of constraints equals the number of variables in a generic closed 3D polyhedron, a shaky polyhedron is a non-trivial singular polyhedron. Since the shaky polyhedron must include valley fold lines, we find its initial topology by flipping the edges of a convex polyhedron. Figures 6 and 7 show examples of shaky polyhedra.

5. Finitely foldable quadrivalent mesh from crease pattern

It is known that a quadrivalent mesh with planar facets with developability and flat-foldability is finitely transformable if there exists an intermediate 3D state [9]; the limitation of this method was that we needed to start from a valid 3D configuration, instead of a 2D crease pattern. By applying Eq. (10) for each interior vertex instead of the existence of 3D state, we can modify a bi-directionally flat-foldable quadrivalent pattern into a finite rigid foldable pattern (Fig. 8). An interesting side effect of using this method for designing discrete version of curved folding represented as planar quad mesh is that the smoothness of the folding is naturally obtained. This successfully avoids the jaggy artifacts that existed in the discrete curved folding representation in [10].

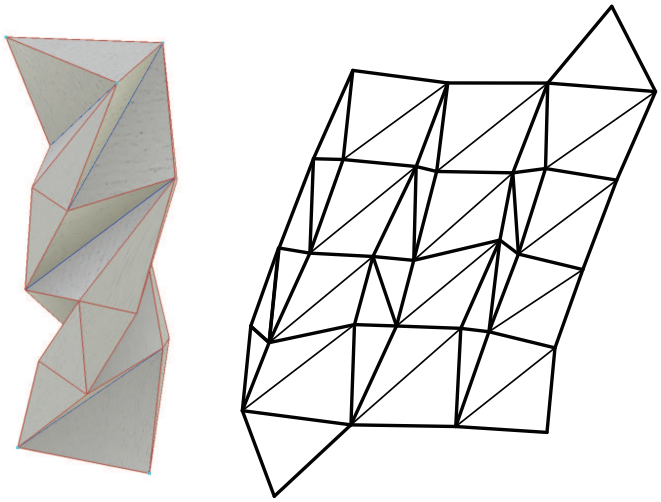

Figure 7: A shaky closed polyhedral tower with partial developability (the entire surface is developable except for the top and bottom vertices indicated in the figure). This polyhedron produces a twisting motion when it is compressed.

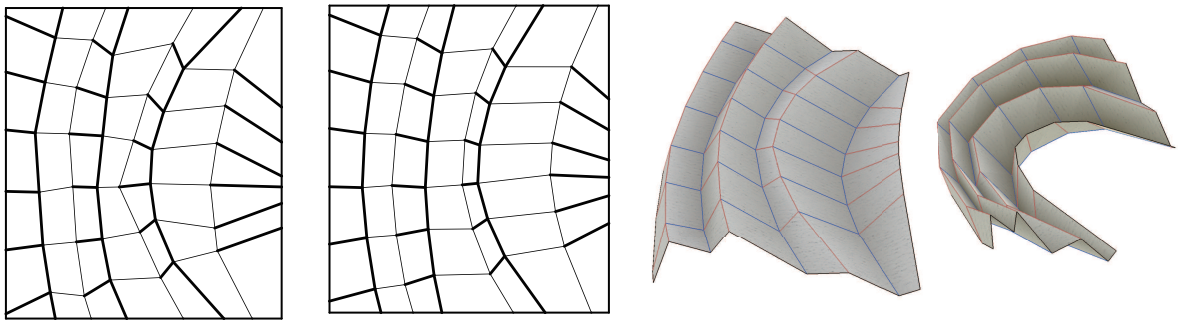

Figure 8: (a) An invalid pattern that satisfies developability and flat-foldability. (b) A valid finitely foldable pattern is obtained when Eq. (10) is introduced. The method also achieves the "smoothness" of discretized curved folding.

6. Origami and tensegrity

The equivalence of an infinitesimal folding mode of a polyhedral surface and the equilibrium of forces implies that the same shape can be used as a shaky polyhedron as well as a tensegrity structure. First-order flexible closed polyhedron is associated with a self-equilibrium form such as a tensegrity structure. By substituting mountain and valley folds of a polyhedron by cables and struts, i.e., compression and tension members, respectively, we can often (but not always) obtain a tensegrity structure where axial forces proportional to the folding angle velocity are applied (Fig. 9). In order to ensure that it is a tensegrity structure, we have to take into account stability along with equilibrium when designing tensegrity structure; this is not the scope of this paper. This graphical connection among different structural systems is an interesting aspect to be investigated in future.

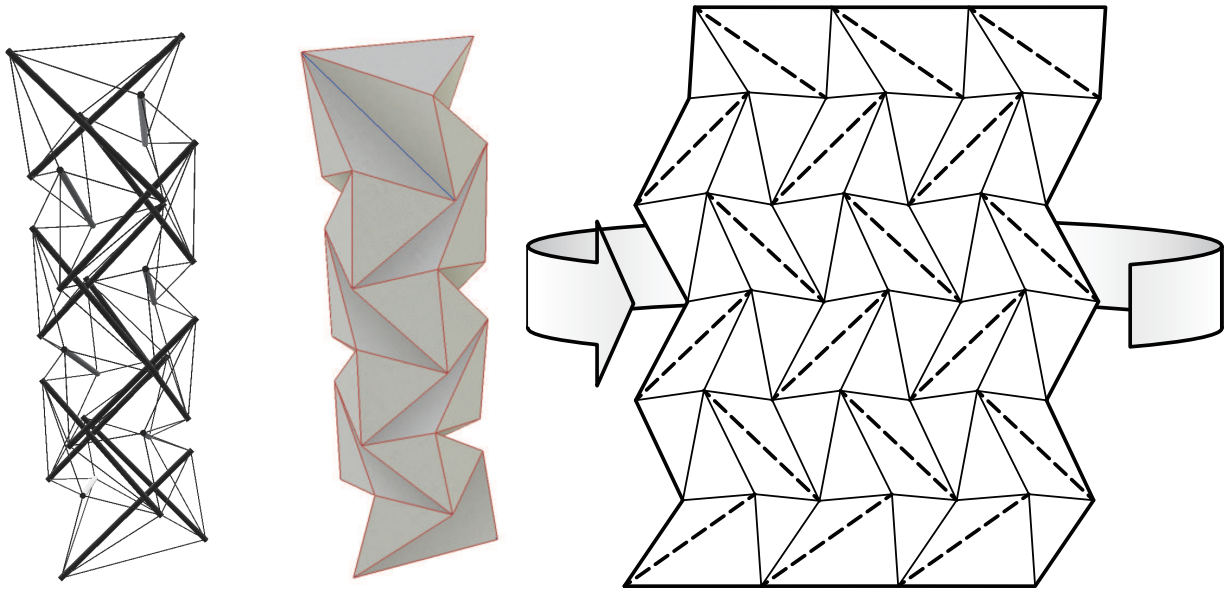

Figure 9: Tensegrity structure vs. shaky polyhedron with its crease pattern.

7. Conclusion

The condition for a valid infinitesimal folding mode of an origami structure homeomorphic to a disk and its equivalence to the edge lengths of its reciprocal figure were demonstrated. In the case of an origami structure with holes, additional three conditions are introduced for each hole. The conditions around each interior vertex and hole are equivalent to the equilibrium conditions of a point and a rigid body, respectively. We also showed the condition that represents infinitesimal foldability when the structure is unfolded flat. We proposed a design system in which an infinitesimally transformable polyhedral surface can be designed interactively by combining with the framework of freeform origami. By using this system, we were able to design variations of shaky closed polyhedron with or without partial developability and finitely rigid foldable quadrivalent origami or discrete curved folding. The potential applications of these models include the design of deployable structures using finite foldability and the designs of energy absorption devices using infinitesimal transformability.

Acknowledgments

This work was supported by the JST Presto program. I would like to thank anonymous reviewers for helpful comments and suggestions.

References

[1] P. Ash, E. Bolker, H. Crapo, W. Whiteley: *Convex polyhedra, dirichlet tessellations, and spider webs*. In *Shaping space*, Birkhäuser 1988, pp. 231–250.

[2] S.-M. Belcastro, T. Hull: *A mathematical model for non-flat origami*. In *Origami*^{3}, Proceedings of the 3rd International Meeting of Origami Mathematics, Science, and Education, 2002, pp. 39–51.

[3] R. Connelly: *A flexible sphere*. The Mathematical Intelligencer **1** (3), 130–131 (1978).

[4] T. Kawasaki: *On the relation between mountain-creases and valley-creases of a flat origami*. In H. Huzita (ed.): Proceedings of the 1st International Meeting of Origami Science and Technology, 1989, pp. 229–237.

[5] J.C. Maxwell: *On reciprocal figures and diagrams of forces*. Philosophical Magazine **27**, 250–261 (1864).

[6] R. Sauer: *Differenzengeometrie*. Springer, 1970.

[7] W.K. Schief, A.I. Bobenko, T. Hoffmann: *On the integrability of infinitesimal and finite deformations of polyhedral surfaces*. In *Discrete Differential Geometry* (Oberwolfach Proceedings), 2007, pp. 67–93.

[8] H. Stachel: *A kinematic approach to Kokotsakis meshes*. Comput.-Aided Geom. Design **27**, 428–237 (2010).

[9] T. Tachi: *Generalization of rigid-foldable quadrilateral-mesh origami*. Journal of the International Association for Shell and Spatial Structures **50** (3), 173–179 (2009).

[10] T. Tachi: *Freeform variations of origami*. J. Geometry Graphics **14** (2), 203–215 (2010).

[11] N. Watanabe, K. Kawaguchi: *The method for judging rigid foldability*. In R. Lang (ed.): *Origami*^{4}*:* The Fourth International Conference on Origami in Science, Mathematics, and Education, A.K. Peters 2009, pp. 165–174.

Received August 2, 2012; final form December 13, 2012